

# $1s2s2p^23p\ ^6L-1s2p^33p\ ^6P$ transitions in O IV, F V and Ne VI

Bin Lin<sup>1</sup>, H Gordon Berry<sup>1</sup>, Tomohiro Shibata<sup>1</sup>, A Eugene Livingston<sup>1</sup>,  
Henri-Pierre Garnir<sup>2</sup>, Thierry Bastin<sup>2</sup> and J Désesquelles<sup>3</sup>

<sup>1</sup> Department of Physics, University of Notre Dame, Notre Dame, IN 46556, USA

<sup>2</sup> IPNAS, University of Liege, B4000 Liege, Belgium

<sup>3</sup> Lab Spectrometrie Ion & Mol, University of Lyon, F-69622 Villeurbanne, France

E-mail: [blin@nd.edu](mailto:blin@nd.edu) and [Berry.20@nd.edu](mailto:Berry.20@nd.edu)

Received 6 April 2004

Published 21 June 2004

Online at [stacks.iop.org/JPhysB/37/2797](http://stacks.iop.org/JPhysB/37/2797)

doi:10.1088/0953-4075/37/13/014

## Abstract

We present observations of VUV transitions between doubly excited sextet states in O IV, F V and Ne VI. Spectra were produced by collisions of an  $O^+$ ,  $(FH)^+$  and  $Ne^+$  beam with a thin carbon foil target. Some observed lines are assigned to the  $1s2s2p^23p\ ^6L-1s2p^33p\ ^6P$  electric-dipole transitions in O IV, F V and Ne VI, and are compared with the results of multi-configuration Hartree–Fock (with QED and higher-order corrections) and multi-configuration Dirac–Fock calculations. 31 new lines have been identified. The sextet systems of boronlike ions are possible candidates for x-ray and VUV lasers.

## 1. Introduction

The sextet systems of boronlike ions are possible candidates for x-ray and VUV lasers [1] and have been investigated recently. The lowest terms of these systems ( $1s2s2p^3\ ^6S$ ,  $1s2s2p^23s\ ^6P$  and  $1s2s2p^33d\ ^6P$ ) have been studied along the B I isoelectronic sequence [2–4]. Studies of a higher excited sextet state ( $1s2p^33s\ ^6S$ ) have been reported recently [1]. However, energy level diagrams of these ions are still far from complete. Experimentally, these levels are difficult to observe by conventional spectroscopic techniques, such as high-voltage discharges in a gas cell, because these levels lie well above several ionization limits of the five-electron singlet states (see figure 1). Even though they are metastable against autoionization, they usually de-excite and disappear by collisions with other ions without radiative transitions. The fast beam–foil technique allows straightforward observations of the radiative transitions produced by these sextet states [5, 6].

In 1992 beam–foil spectroscopy [2] was used to provide initial data on low-lying sextet states in doubly excited boronlike nitrogen, oxygen and fluorine. Recent work of

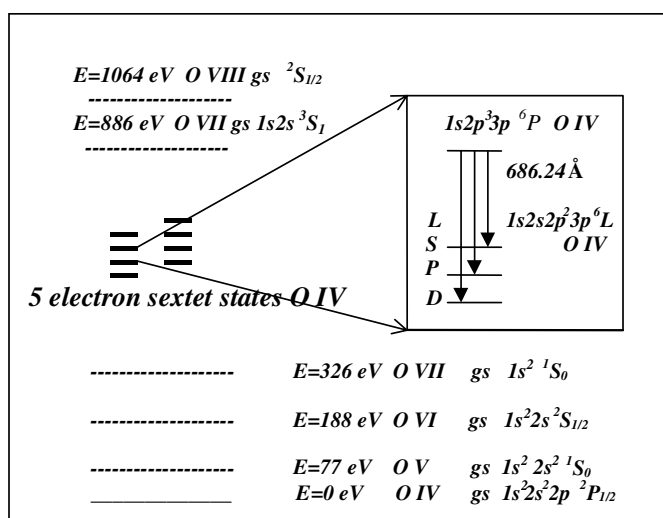


**Figure 1.** Term diagram of the doubly excited sextet states of O IV. The mean wavelength for the  $1s2s2p^23p\ ^6L-1s2p^33p\ ^6P^o$  transitions in O IV is shown.

Lapierre and Knystautas [3] on possible sextet transitions in Ne VI highlights the significance of this sequence. They measured several excitation energies and lifetimes. Fine structures of the  $1s2s2p^23s\ ^6P_J$  states were resolved and measured in O IV, F V and Ne VI by Lin *et al* [1]. There are no further results reported for transitions from highly excited sextet states.

In some beam-foil spectroscopic studies of sextet states in the B I isoelectronic sequence, rather weak lines and overwhelming blending problems are found. Hence, accurate theoretical studies of sextet states in the B I isoelectronic sequence are strongly needed to help identifications. However, theoretical analysis of these five-electron systems is difficult because strong electron correlation, relativistic corrections and even quantum electrodynamic (QED) effects have to be included in the calculations [4, 1, 7]. Recent line identifications in the sextet systems were made on the basis of multi-configuration Hartree-Fock (MCHF) (with QED and higher-order corrections [1], the latter are higher-order corrections not included in the MCHF calculation as compared to the MCDF method [1]) and multi-configuration Dirac-Fock (MCDF) calculations [2, 4, 1, 8] or on the basis of Z-expansion along the B I isoelectronic sequence [3, 1]. From these works six terms have been determined.

The sextet states  $1s2s2p^23p\ ^6L$ ,  $L = S, P, D$  and  $1s2p^33p\ ^6P$  in the B I isoelectronic sequence are well above several ionization levels as shown in figure 1. Many levels are metastable against electric-dipole radiative decay to singly excited five-electron states and against Coulomb autoionization into the adjacent continuum  $1s^22l'2l''nl\ ^4L$  due to different spin multiplicity. Thus, the main decay channel is by radiation in the fast beam-foil experiments.

In this work, fast beam-foil spectra of oxygen were recorded at Liege using grating spectrometers. Similar spectra of fluorine and neon were previously recorded at the University of Lyon and at the Argonne National Laboratory. The  $1s2s2p^23p\ ^6L-1s2p^33p\ ^6P$ ,  $L = S, P, D$  electric-dipole transitions in O IV, F V and Ne VI have been searched for in these spectra. Comparisons are given with the results from the MCHF calculations (with QED and higher-order corrections [1]) and from the MCDF calculations.

## 2. Theory

The MCHF method [8] with QED and higher-order relativistic corrections [1, 12–14] and the MCDF GRASP code [9–11] support the analysis of the above experimental spectra.

In the MCHF approach, for a sextet state in a five-electron system  $(\beta, LS = 5/2JM_J) = (n_1l_1^{w_1}n_2l_2^{w_2}n_3l_3^{w_3}n_4l_4^{w_4}n_5l_5^{w_5} {}^6L_J, M_J)$ , where  $w_i = 0, 1, \dots, \min(2l_i + 1)$ ,  $i = 1, 2, \dots, 5$ , the wavefunction is

$$\Psi(\beta, LS = 5/2J) = \sum_{i=1}^N \sum_{M_J=-J}^J c_i \phi(\beta_i, LS = 5/2JM_J), \quad (1)$$

where  $c_i$  is a configuration interaction coefficient,  $N$  is the total number of configurations with the same  $LSJM_J$  and parity, and  $\phi(\beta_i, LS = 5/2JM_J)$  is a configuration state function (CSF).

Firstly, the single-configuration Hartree–Fock (SCHF) calculations where configurations are the desired levels, i.e., 1s2s2p<sup>2</sup>3p or 1s2p<sup>3</sup>3p, were performed. After updating the MCHF codes, we carried out relativistic calculations with an initial expansion of up to 4000 CSFs and a full Pauli–Breit Hamiltonian matrix. For a five-electron system a CI expansion generated by an active set leads to a large number of expansions. To reduce the number of configurations, we chose configurations  $n_1l_1^{w_1}n_2l_2^{w_2}n_3l_3^{w_3}n_4l_4^{w_4}n_5l_5^{w_5}$ , where  $n_i = 1, 2, 3, 4$  and  $5$ ,  $l_i = 0, \dots, \min(4, n_i - 1)$ . We did not include  $g$  electrons for the  $n = 5$  shell. For the MCHF calculations of the lower states 1s2s2p<sup>2</sup>3p <sup>6</sup>L,  $L = S, P, D$ , we chose 1s, 2s, 2p, 3s, 3p, 3d, 4s, 4p, 4d and 5s electrons to compose the configurations. For the 1s2p<sup>3</sup>3p <sup>6</sup>P state we chose 1s through 4d electrons. Fine structure splitting is strongly involved in the experiments and identifications. After determining radial wavefunctions, we included relativistic operators of mass correction, one- and two-body Darwin terms and spin–spin contact term in both SCHF and MCHF calculations; these were not included in early work of Miecznik *et al* [4].

In addition, we used the screened hydrogenic formula from [1, 12–14] to estimate QED, and higher-order relativistic contributions for sextet states in five-electron oxygen, fluorine and neon.

In the MCDF [9–11] approach, firstly, we used the single-configuration Dirac–Fock (SCDF) approach. A basis of  $jj$ -coupled states to all possible total angular momenta  $J$  from two non-relativistic configurations, 1s2s2p<sup>2</sup>3p and 1s2p<sup>3</sup>3p, was considered. For convergence we included the ground state 1s<sup>2</sup>2s<sup>2</sup>2p of the five-electron systems. After calculating all possible levels for all  $J$ , eigenvectors were regrouped in a basis of  $LS$  terms. To obtain better evaluations of correlation energies of the sextet terms 1s2s2p<sup>2</sup>3p <sup>6</sup>L,  $L = S, P, D$  and 1s2p<sup>3</sup>3p <sup>6</sup>P in O IV, F V and Ne VI, improved calculations included 1s<sup>2</sup>2s<sup>2</sup>2p, 1s<sup>2</sup>2s2p<sup>2</sup>, 1s2s<sup>2</sup>2p<sup>2</sup>, 1s2s2p<sup>3</sup>, 1s2s2p<sup>2</sup>3s, 1s2s2p<sup>2</sup>3p, 1s2s2p<sup>2</sup>3d, 1s2p<sup>3</sup>3s, 1s2p<sup>3</sup>3p, 1s2p<sup>3</sup>3d, 1s2p<sup>3</sup>4s, 1s2p<sup>3</sup>4p and 1s2p<sup>3</sup>4d mixing non-relativistic configurations.

In the GRASP code the QED effects, self-energy and vacuum polarization correction were taken into account by using an effective nuclear charge  $Z_{\text{eff}}$  in the formulae of QED effects, from an analogous hydrogenic orbital with the same expectation value of  $r$  as the MCDF-orbital in question [9–11].

## 3. Experiment

The experiments were performed on a standard fast beam–foil excitation system at a Van de Graaff accelerator beam line at the University of Liege [6, 15–18]. To produce spectra of oxygen in the wavelength region near 660–710 Å, a beam current of about 1.3 μA of <sup>32</sup>O<sub>2</sub><sup>+</sup> and

$^{16}\text{O}^+$  ions at beam energies of 1.5 and 1.7 MeV was used. Such energies were expected to be optimum for comparison and production of  $\text{O}^{3+}$  ions by ion–foil interaction [19].

The beam current goes through a carbon exciter foil. The foils were made using a glow discharge, had surface densities of about  $10\text{--}20\ \mu\text{g cm}^{-2}$  and lasted for 1–2 h under the above bombardment.

VUV radiation emitted by excited oxygen ions was dispersed by a 1 m Seya-Namioka grating-incidence spectrometer at about  $90^\circ$  to the ion beam direction. A low-noise channeltron (below  $1\ \text{count min}^{-1}$ ) served as a detector. Spectra were recorded at energies of 1.5 and 1.7 MeV with  $100/100\ \mu\text{m}$  slits (the linewidth (FWHM) was  $1.1\ \text{\AA}$ ) and  $40/40\ \mu\text{m}$  slits (the linewidth (FWHM) was  $0.7\ \text{\AA}$ ) in the wavelength range of  $660\text{--}710\ \text{\AA}$ .

We also reinvestigated unpublished beam–foil spectra of  $^{16}\text{O}^{3+}$ ,  $^{19}\text{F}^{4+}$  and  $^{20}\text{Ne}^{5+}$  ions recorded previously by accelerating  $^{16}\text{O}^+$ ,  $^{20}(\text{FH})^+$  and  $^{20}\text{Ne}^+$  ions to energies of 2.5 MeV, 2.5 MeV and 4.0 MeV at the University of Lyon and at the Argonne National Laboratory. The linewidths (FWHM) were  $0.4\ \text{\AA}$ ,  $0.8\ \text{\AA}$  and  $0.3\ \text{\AA}$  in the wavelength ranges of  $660\text{--}710\ \text{\AA}$ ,  $560\text{--}640\ \text{\AA}$  and  $490\text{--}540\ \text{\AA}$  in the above spectra, respectively.

#### 4. Results

Figures 2(a)–(c) display three typical spectra of oxygen at beam energies of 1.5, 1.7 and 2.5 MeV in the wavelength range of  $660\text{--}705\ \text{\AA}$ . In the wavelength region of  $665\text{--}675\ \text{\AA}$  the  $1s2s2p^23p\ ^6\text{D}^\circ\text{--}1s2p^33p\ ^6\text{P}$  transitions in O IV were expected. At an  $\text{O}_2^+$  beam energy of 1.5 MeV,  $\text{O}_2^+$  ions are mainly excited to terms of  $\text{O}^{2+}$  and  $\text{O}^{3+}$ . There are no lines emitted from sextet states in O IV in figure 2(a). At an  $\text{O}^+$  beam energy of 1.7 MeV,  $\text{O}^+$  ions are mainly excited to terms of  $\text{O}^{3+}$  and  $\text{O}^{4+}$ . New and unidentified emissions appear in the spectrum in figure 2(b). Figure 2(c) shows a spectrum with better resolution to see details of lines. For the  $1s2s2p^23p\ ^6\text{L}^\circ\text{--}1s2p^33p\ ^6\text{P}$ ,  $L = \text{S, P, D}$  transitions we expected to partially resolve fine structures of the lower states  $1s2s2p^23p\ ^6\text{L}_j^\circ$ ,  $L = \text{S, P, D}$  in the experiments, whereas fine structures of the upper state  $1s2p^33p\ ^6\text{P}_j$  are small and less than the resolution of the experimental spectra. A promising candidate for the  $1s2s2p^23p\ ^6\text{D}_{9/2}^\circ\text{--}1s2p^33p\ ^6\text{P}_{7/2}$  transition at  $668.95 \pm 0.08\ \text{\AA}$  appears in the spectra recorded at 1.7 and 2.5 MeV  $\text{O}^+$  ion beam energies (labelled as D in figures 2(b) and (c)), and does not appear in the spectrum recorded at 1.5 MeV  $\text{O}_2^+$  ion beam energy. Well-known transitions of O V  $3p\text{--}4d$ , O IV  $2s^23p\text{--}2s^25s$ , O V  $2s3d\text{--}2s4f$  and O III  $2s^22p^2\text{--}2s2p^3$  are at  $659.589\ \text{\AA}$ ,  $670.601\ \text{\AA}$ ,  $681.332\ \text{\AA}$  and  $703.854\ \text{\AA}$  respectively, close to the neighbourhood of the doubly excited sextet transitions. The four wavelengths have been semiempirically fitted with an accuracy of  $\pm 0.004\ \text{\AA}$  in [20–22] and provided a good calibration for the measurements. Standard error for the wavelength calibration is  $0.01\ \text{\AA}$  in the region of  $660\text{--}710\ \text{\AA}$ . Nonlinear least-squared fittings of Gaussian profiles gave values for wavelengths, intensities and full widths at half maximum (FWHM) of lines. Uncertainties of wavelengths are related to intensities of the lines. Through the use of optical refocusing we achieved spectroscopic linewidths of  $0.7$  and  $0.4\ \text{\AA}$  in figures 2(b) and (c). The precision of the profile-fitting program was checked through several known transition wavelengths.

Most new identifications have been obtained by searching in the spectra for sets of unidentified lines and by comparing energies and relative intensities of the  $1s2s2p^23p\ ^6\text{L}^\circ\text{--}1s2p^33p\ ^6\text{P}$ ,  $L = \text{D, P and S}$ , transitions with the results calculated by the MCHF and the MCDF approaches. Figure 3(a) shows details of the  $1s2s2p^23p\ ^6\text{D}^\circ\text{--}1s2p^33p\ ^6\text{P}$  transition in O IV recorded at an  $\text{O}^+$  ion energy of 2.5 MeV. The curve ‘SCHF’ is the convoluted theoretical profile of fine structure components with a Gaussian function. The experimental width of

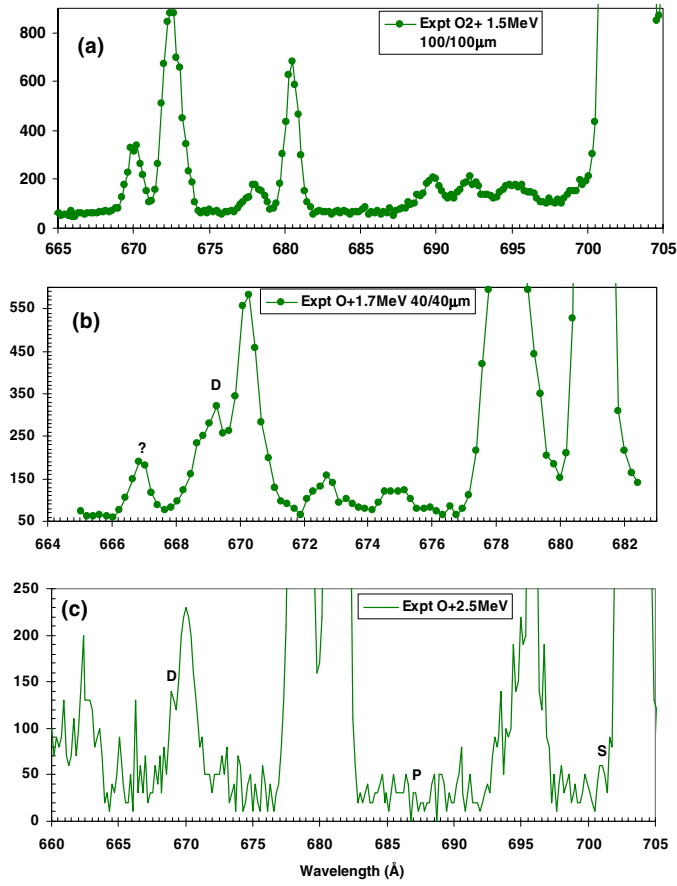


**Figure 2.** Beam-foil spectra of oxygen, recorded at different energies. The units of intensities are arbitrary. Beam energies and spectrometer slit widths (in  $\mu\text{m}$ ) are indicated. D, P and S:  $1s2s2p^23p$   ${}^6L_{J'}^o-1s2p^33p$   ${}^6P_{J'}$ , L = D, P and S transitions in O IV.

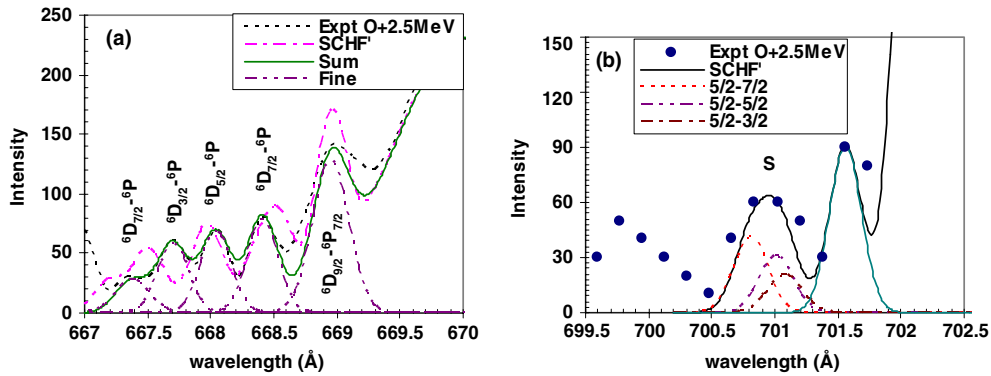


**Figure 3.** Relative intensities of the  $1s2s2p^23p$   ${}^6D_{J'}^o-1s2p^33p$   ${}^6P_{J'}$  and  $1s2s2p^23p$   ${}^6S_{3/2}^o-1s2p^33p$   ${}^6P_{J'}$  transitions of O IV in the experimental spectrum of oxygen at the energy of 2.5 MeV. The units of intensities are arbitrary.

0.4 Å for the oxygen spectrum was utilized. The transition rates to the fine structures  $J = 9/2$  through  $3/2$  of the lower state were the results of the SCHF calculations by this work. The wavelengths of the fine structure components were the calculated SCHF results plus a fitted shift for all five components. The measured wavelength of a component is the weighted centre of the fitted profile of the experimental data. Experimental transition rate is proportional to area of a peak (fitted intensity  $\times$  FWHM of the experimental data). The curve ‘sum’ is the summation of the fitted fine structure components of the experimental data. The measured ratio of the  $J = 9/2-7/2$ ,  $J = 7/2-*$ ,  $J = 5/2-*$ ,  $J = 3/2-*$  and  $J = 1/2-*$  transition rates at an ion energy of 2.5 MeV in figure 3(a) is about  $(121 \times 0.4):(76 \times 0.4):(66 \times 0.4):(55 \times 0.4):(27 \times 0.4) = 4.79:2.92:2.58:2.19:1.00$ . \* represents all possible allowed  $J$  of the upper state  $1s2p^33p\ ^6P_J$ . The ratio is slightly different from the theoretical ratio of the  $gf$  values from the SCHF calculations,  $0.981:0.593:0.530:0.355:0.294 = 4.98:3.99:3.00:2.00:1.00$ . Based on the above analysis we assign the set of lines as the  $1s2s2p^23p\ ^6D^o-1s2p^33p\ ^6P$  transition in O IV, and determine their wavelengths with a good accuracy of  $\pm 0.08$  Å. The results are listed in table 1. The strongest transition related to fine structure components is the  $1s2s2p^23p\ ^6D_{9/2}^o-1s2p^33p\ ^6P_{7/2}$  transition at the wavelength of  $668.95 \pm 0.08$  Å.

Spectral details of the  $1s2s2p^23p\ ^6S_{5/2}^o-1s2p^33p\ ^6P_J$  transition are shown in figure 3(b). The width of the line is wider than the experimental width of a resonance line of 0.4 Å, but not wide enough to resolve fine structures of the upper state  $1s2p^33p\ ^6P$ . In the experimental profile, experimental separation of the fine structures of the upper state appears larger than the results of the SCHF calculations. Similar to above, after studying details of the transitions theoretically and experimentally, and comparing with the MCHF and the MCDF calculations of O IV in this work, we were able to assign these unidentified observed lines the  $1s2s2p^23p\ ^6L^o-1s2p^33p\ ^6P$ ,  $L = D, P$  and  $S$ , electric-dipole transitions in O IV. Results of the identifications and the measurements of the wavelengths of the transitions are listed in table 1. Errors of the wavelengths of  $\pm 0.08$  Å are small, which result mainly from the calibration and the curve fitting. The latter includes experimental and statistical errors. In table 1 the average theoretical transition energy  $AV$  is the centre of gravity of the  $1s2s2p^23p\ ^6L^o-1s2p^33p\ ^6P$  transition energies (computed from the calculated fine structure lines by this work) with the results of theoretical analysis. The experimental transition energy  $AV$  is the centre of gravity of the  $1s2s2p^23p\ ^6L^o-1s2p^33p\ ^6P$  transition energies (computed from the observed lines) with the results of experimental transition rate analysis.  $AV^T$  is the summation of the above average transition energy ( $AV$ ), the QED effect (QED) and the higher-order correction (HO). Errors for the calculated transition energies in table 1 are the root mean squared differences between the calculated and the experimental transition energies as given in the table. We also list calculated non-relativistic transition energies (N-REL). In table 1 we present the measured fine structure wavelength values and compare these with different theoretical values for O IV. The experimental results are consistent with the calculations after considering the experimental and the theoretical errors.

Using similar experimental and theoretical analyses described, we have studied spectra recorded at a  $(FH)^+$  beam energy of 2.5 MeV. Through the use of optical refocusing we achieved a spectroscopic linewidth of 0.7 Å. The wavelength accuracy is  $\pm 0.10$  Å in the wavelength region of 570–620 Å in the spectra [23, 24]. In table 2 all observed lines in the sextet system of F V are reported. Nine lines are new observations. For the  $1s2s2p^23p\ ^6L-1s2p^33p\ ^6P$  transitions fine structures of the lower state  $1s2s2p^23p\ ^6L$  are resolved in the experiments. The strongest fine structure component is the  $1s2s2p^23p\ ^6D_{9/2}^o-1s2p^33p\ ^6P_{7/2}$  transition at the wavelength of  $577.50 \pm 0.10$  Å.

**Table 1.** Energies  $E$  (in  $\text{cm}^{-1}$ ) and wavelengths  $\lambda$  (in  $\text{\AA}$ ) for the  $1s2s2p^23p^6L_J-1s2p^33p^6P_{J'}$  transitions in O IV in this work. \* represents all possible allowed  $J$  of the upper states by the E1 transition selection rule. We list energy difference  $dE$  (in  $\text{cm}^{-1}$ ) between theoretical and experimental transition energies for the  $1s2s2p^23p^6L_J-1s2p^33p^6P_{J'}$  transitions.

$J-J'$	$\lambda_{\text{EXP}}$	$E_{\text{EXP}}$	$\lambda_{\text{MCHF}}$	$E_{\text{MCHF}}$	$dE_{\text{MCHF}}$	$\lambda_{\text{SCHF}}$	$E_{\text{SCHF}}$	$dE_{\text{SCHF}}$	$\lambda_{\text{MCDF}}$	$E_{\text{MCDF}}$	$dE_{\text{MCDF}}$	$\lambda_{\text{SCDF}}$	$E_{\text{SCDF}}$	$dE_{\text{SCDF}}$
	$\pm 0.08$													
	$1s2s2p^23p^6D_J^o-1s2p^33p^6P_{J'}$													
				$\pm 32$			$\pm 372$		$\pm 710$			$\pm 1938$		
1/2-*	667.26	149 867	667.36	149 844	-22	668.82	149 517	-350	664.15	150 568	702	658.84	151 782	1915
3/2-*	667.70	149 768	667.68	149 772	4	669.12	149 450	-318	664.58	150 471	703	659.12	151 717	1950
5/2-*	668.04	149 692	668.13	149 671	-20	669.59	149 345	-347	665.00	150 376	684	659.59	151 609	1918
7/2-*	668.41	149 609	668.54	149 580	-29	670.10	149 231	-377	665.64	150 231	623	660.11	151 490	1881
9/2-7/2	668.95	149 488	669.07	149 461	-27	670.57	149 127	-361	666.27	150 089	601	660.62	151 373	1885
AV	668.34	149 623	668.44	149 602	-22	669.94	149 267	-356	665.48	150 267	644	660.66	151 364	1740
QED				-23.6			-23.4							
HO				139.6			-16.7							
AV <sup>T</sup>			667.92	149 718	95	670.12	149 227	-396						
N-REL						673.61	148 453	-1170						
	$1s2s2p^23p^6P_J^o-1s2p^33p^6P_{J'}$													
				$\pm 258$			$\pm 555$		$\pm 1782$			$\pm 677$		
3/2-*	687.14	145 531	685.95	145 785	255	684.51	146 090	559	678.94	147 288	1758	675.90	147 951	2420
5/2-*	687.35	145 486	686.23	145 724	237	685.04	145 977	491	679.15	147 243	1757	676.18	147 890	2403
7/2-*	687.65	145 423	686.69	145 626	203	685.25	145 932	509	679.91	147 078	1655	676.76	147 763	2340
AV	687.44	145 468	686.37	145 694	226	685.02	145 982	514	679.44	147 180	1712	676.38	147 847	2379
QED				-23.5			-23.3							
HO				29.1			-39.1							
AV <sup>T</sup>			686.34	145 700	232	685.31	145 920	452						
N-REL						688.66	145 209	-259						
	$1s2s2p^23p^6S_J^o-1s2p^33p^6P_{J'}$													
				$\pm 7507$			$\pm 771$		$\pm 4252$			$\pm 5880$		
5/2-*	700.93	142 668	739.86	135 161	-7507	704.74	141 896	-771	722.46	134 216	-4252	731.06	136 788	-5880
QED				-23.0			-23.1							
HO				149.3			66.7							
AV <sup>T</sup>			739.17	135 287	-7381	704.53	141 940	-728						
N-REL						708.76	141 091	-1576						

**Table 2.** Energies  $E$  (in  $\text{cm}^{-1}$ ) and wavelengths  $\lambda$  (in  $\text{\AA}$ ) for the  $1s2s2p^23p\ ^6L_J^o-1s2p^33p\ ^6P_{J'}$  transitions in F V in this work. \* represents all possible allowed  $J$  of the upper states by the E1 transition selection rule. We list differences  $dE$  (in  $\text{cm}^{-1}$ ) between theoretical and experimental transition energies for the  $1s2s2p^23p\ ^6L_J^o-1s2p^33p\ ^6P_{J'}$  transitions.

$J-J'$	$\lambda_{\text{EXP}}$	$E_{\text{EXP}}$	$\lambda_{\text{MCHF}}$	$E_{\text{MCHF}}$	$dE_{\text{MCHF}}$	$\lambda_{\text{SCHF}}$	$E_{\text{SCHF}}$	$dE_{\text{SCHF}}$	$\lambda_{\text{MCDF}}$	$E_{\text{MCDF}}$	$dE_{\text{MCDF}}$	$\lambda_{\text{SCDF}}$	$E_{\text{SCDF}}$	$dE_{\text{SCDF}}$	
	$\pm 0.10$														
	$1s2s2p^23p\ ^6D_J^o-1s2p^33p\ ^6P_{J'}$														
				$\pm 1043$			$\pm 328$			$\pm 965$			$\pm 2767$		
1/2-*	575.20	173 853	572.17	174 743	921	576.24	173 539	-314	572.33	174 724	872	566.42	176 547	2695	
3/2-*	575.85	173 656	572.40	174 703	1047	576.61	173 427	-229	572.72	174 605	949	566.77	176 438	2782	
5/2-*	576.43	173 482	573.26	174 441	959	577.23	173 241	-240	573.30	174 429	947	567.46	176 224	2742	
7/2-*	577.09	173 283	573.89	174 249	966	577.95	173 025	-258	574.15	174 171	887	568.49	175 905	2621	
9/2-7/2	577.50	173 160	574.04	174 204	1044	578.66	172 813	-347	575.06	173 895	735	569.01	175 744	2584	
AV	576.80	173 369	573.50	174 368	998	577.75	173 085	-284	573.97	174 225	855	568.09	176 028	2659	
QED				-41.7			-41.4								
HO				211.0			372.5								
AV <sup>T</sup>			572.94	174 537	1168	576.65	173 416	47							
N-REL						582.31	171 729	-1640							
	$1s2s2p^23p\ ^6P_J^o-1s2p^33p\ ^6P_{J'}$														
				$\pm 1084$			$\pm 418$			$\pm 1761$			$\pm 2787$		
3/2-*	592.45	168 791	589.86	169 532	741	591.01	169 202	411	587.55	170 198	1408	582.83	171 577	2786	
5/2-*	592.67	168 728	589.13	169 742	1014	591.26	169 130	402	586.65	170 459	1731	583.17	171 477	2749	
7/2-*	593.43	168 512	589.86	169 532	1020	592.16	168 873	361	587.70	170 155	1643	583.96	171 245	2733	
AV	592.96	168 646	589.62	169 602	956	591.60	169 032	386	587.32	170 266	1620	583.45	171 396	2750	
QED				-41.5			-41.2								
HO				216.2			343.4								
AV <sup>T</sup>			589.01	169 777	1131	590.55	169 334	688							
N-REL						596.37	167 682	-964							
	$1s2s2p^23p\ ^6S_J^o-1s2p^33p\ ^6P_{J'}$														
				$\pm 6116$			$\pm 105$			$\pm 4418$			$\pm 5379$		
5/2-*	615.57	162 451	639.65	156 335	-6116	615.97	162 346	-105	632.82	158 023	-4428	636.65	157 072	-5379	
QED				-40.7			-40.8								
HO				251.1			176.5								
AV <sup>T</sup>			638.79	156 545	-5906	615.45	162 482	31							
N-REL						620.90	161 058	-1393							

**Table 3.** Energies  $E$  (in  $\text{cm}^{-1}$ ) and wavelengths  $\lambda$  (in  $\text{\AA}$ ) for the  $1s2s2p^23p^6L_J^o-1s2p^33p^6P_{J'}$  transitions in Ne in this work. \* represents all possible allowed  $J$  of the upper states by the E1 transition selection rule. We list differences  $dE$  (in  $\text{cm}^{-1}$ ) between theoretical and experimental transition energies for the  $1s2s2p^23p^6L_J^o-1s2p^33p^6P_{J'}$  transitions.

$J-J'$	$\lambda_{\text{EXP}}$	$E_{\text{EXP}}$	$\lambda_{\text{MCHF}}$	$E_{\text{MCHF}}$	$dE_{\text{MCHF}}$	$\lambda_{\text{SCHF}}$	$E_{\text{SCHF}}$	$dE_{\text{SCHF}}$	$\lambda_{\text{MCDF}}$	$E_{\text{MCDF}}$	$dE_{\text{MCDF}}$	$\lambda_{\text{SCDF}}$	$E_{\text{SCDF}}$	$dE_{\text{SCDF}}$
	$\pm 0.05$													
	$1s2s2p^23p^6D_J^o-1s2p^33p^6P_{J'}$													
	$\pm 917$													
	$\pm 557$													
	$\pm 1153$													
	$\pm 3497$													
1/2-3/2	505.20	197 941	502.64	198 950	1008	505.41	197 859	-82	502.07	199 175	1234	496.29	201 495	3554
3/2-*	505.44	197 847	503.19	198 732	885	505.96	197 644	-203	502.50	199 005	1158	496.62	201 361	3514
5/2-*	505.77	197 718	503.87	198 464	746	506.72	197 348	-371	503.40	198 649	931	497.52	200 997	3279
7/2-7/2	506.17	197 562	504.55	198 196	634	507.39	197 087	-475	504.20	198 334	772	498.26	200 698	3136
7/2-5/2	506.50	197 433	504.96	198 035	602	507.78	196 936	-498	504.53	198 204	771	498.67	200 533	3100
9/2-7/2	507.13	197 188	505.78	197 714	526	508.61	196 614	-574	505.47	197 836	648	499.53	200 188	3000
AV	506.29	197 517	504.56	198 192	675	507.38	197 089	-428	504.13	198 361	844	498.23	200 710	3193
QED				-68.2			-66.8							
HO				-220.0			78.9							
AV <sup>T</sup>			505.30	197 904	387	507.35	197 101	-416						
N-REL						512.88	194 977	-2540						
	$1s2s2p^23p^6P_J^o-1s2p^33p^6P_{J'}$													
	$\pm 1190$													
	$\pm 119$													
	$\pm 1832$													
	$\pm 3013$													
3/2-5/2	519.53	192 482	516.38	193 656	1174	519.23	192 593	111	514.98	194 182	1701	511.58	195 473	2991
3/2-3/2	519.77	192 393	516.55	193 592	1199	519.46	192 508	115	515.21	194 096	1703	511.73	195 416	3023
5/2-7/2														
5/2-3/2	520.26	192 212	517.20	193 349	1137	520.06	192 286	74	516.00	193 798	1587	512.32	195 191	2979
7/2-7/2	520.78	192 020	517.81	193 121	1101	520.74	192 034	15	515.64	193 934	1914	512.93	194 958	2939
7/2-5/2	521.36	191 806	518.24	192 961	1155	521.15	191 883	77	517.02	193 416	1610	513.38	194 787	2981
AV	520.35	192 178	517.24	193 333	1156	520.14	192 255	77	515.72	193 903	1726	512.39	195 162	2984
QED				-67.8			-66.5							
HO				-50.3			-10.7							
AV <sup>T</sup>			517.56	193 215	1037	520.35	192 178	0						
N-REL						525.74	190 137	-2041						
	$1s2s2p^23p^6S_J^o-1s2p^33p^6P_{J'}$													
	$\pm 5314$													
	$\pm 735$													
	$\pm 4341$													
	$\pm 4617$													
5/2-7/2	548.62	182 276	564.89	177 026	-5250	546.46	182 996	720	561.94	177 955	-4321	562.50	177 778	-4498
5/2-5/2,3/2	548.94	182 169	565.40	176 866	-5303	546.99	182 819	649	562.33	177 832	-4338	563.15	177 573	-4597
AV	548.80	182 216	565.17	176 937	-5280	546.75	182 897	681	562.16	177 886	-4330	562.86	177 664	-4553
QED				-66.7			-66.7							
HO				-165.6			16.5							
AV <sup>T</sup>			565.92	176 705	-5511	546.91	182 847	631						
N-REL						553.04	180 817	-1459						

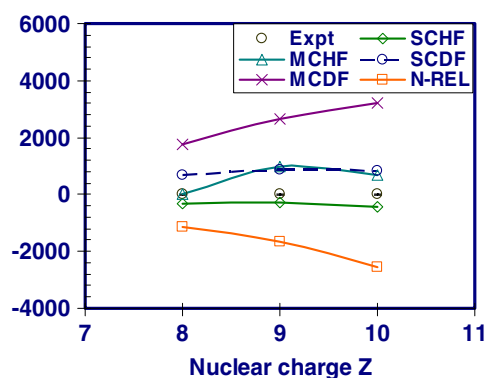


**Figure 4.** Differences between the theoretical and the experimental transition energies for the  $1s2s2p^2 3p \ ^6D^o - 1s2p^3 3p \ ^6P$  transitions. The unit of energy difference is  $\text{cm}^{-1}$ .

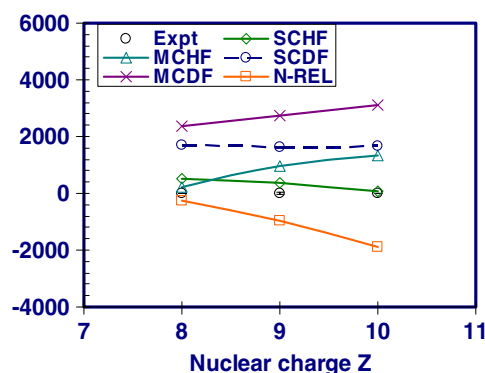


**Figure 5.** Differences between the theoretical and the experimental transition energies for the  $1s2s2p^2 3p \ ^6P^o - 1s2p^3 3p \ ^6P$  transitions. The unit of energy difference is  $\text{cm}^{-1}$ .

Similarly, we have studied spectra recorded at a  $\text{Ne}^+$  beam energy of 4.0 MeV. Through the use of optical refocusing, a spectroscopic linewidth of 0.3 Å was achieved in the second-order spectra. Fine structures of the lower and upper states are resolved. The wavelength accuracy is  $\pm 0.05$  Å for the  $1s2s2p^2 3p \ ^6L^o - 1s2p^3 3p \ ^6P^o$ ,  $L = S, P, D$ , transitions in the wavelength region of 490–555 Å [25, 26]. In table 3, 13 new observed lines in the sextet system of Ne VI are reported. The strongest fine structure component is the  $1s2s2p^2 3p \ ^6D^o_{9/2} - 1s2p^3 3p \ ^6P^o_{7/2}$  transition at the wavelength of  $507.13 \pm 0.05$  Å.

In figures 4, 5 and 6 we show differences between theoretical and experimental transition energies of the  $1s2s2p^2 3p \ ^6L^o - 1s2p^3 3p \ ^6P$ ,  $L = D, P, S$ , transitions along the boronlike isoelectronic sequence. Here, the theoretical transition energy is the centre of gravity of the  $1s2s2p^2 3p \ ^6L^o - 1s2p^3 3p \ ^6P$  transition energies (computed from the calculated fine structure lines by this work) with the results of theoretical analysis, and the experimental transition energy is the centre of gravity of the  $1s2s2p^2 3p \ ^6L^o - 1s2p^3 3p \ ^6P$  transition energies (computed from the observed lines) with the experimental results of transition rate analysis.

In figure 4 the calculated SCHF and SCDF transition energy differences from the experiments are constant for the  $1s2s2p^2 3p \ ^6D^o - 1s2p^3 3p \ ^6P$  transitions for nuclear charges  $Z = 8, 9$  and 10. For the MCDF and the non-relativistic SCHF calculations, the differences

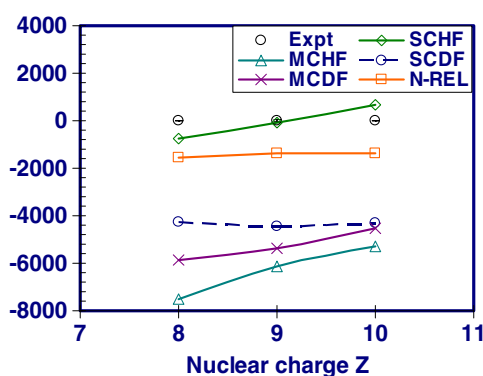


Figure 6. Differences between the theoretical and the experimental transition energies for the 1s2s2p<sup>2</sup>3p <sup>6</sup>S<sup>o</sup>–1s2p<sup>3</sup>3p <sup>6</sup>P transitions. The unit of energy difference is cm<sup>-1</sup>.

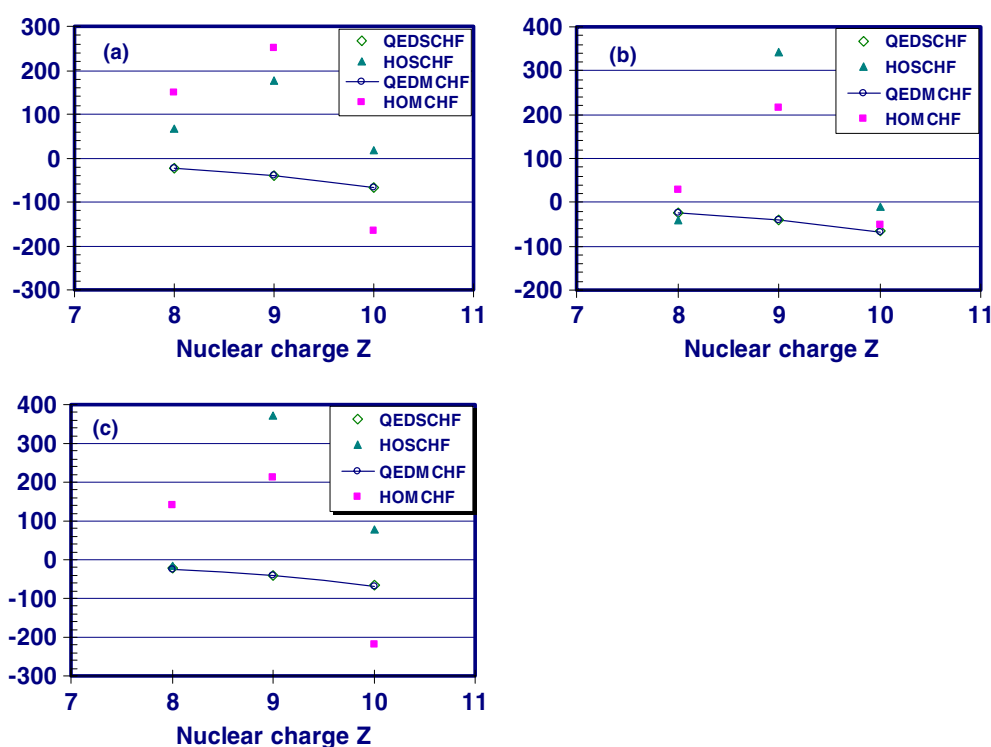


Figure 7. Isoelectronic comparison of the QED and the higher-order corrections of the (a) 1s2s2p<sup>2</sup>3p <sup>6</sup>D<sup>o</sup>–1s2p<sup>3</sup>3p <sup>6</sup>P, (b) 1s2s2p<sup>2</sup>3p <sup>6</sup>P<sup>o</sup>–1s2p<sup>3</sup>3p <sup>6</sup>P and (c) 1s2s2p<sup>2</sup>3p <sup>6</sup>S<sup>o</sup>–1s2p<sup>3</sup>3p <sup>6</sup>P transitions for the B I sequence. The QED effects from the SCHF and MCHF calculations are denoted by solid lines. The units of energies are cm<sup>-1</sup>.

are linear for nuclear charges  $Z = 8, 9$  and  $10$ . For the MCHF calculations for oxygen, the difference is very small, just  $22 \text{ cm}^{-1}$ .

In figure 5 the SCDF difference is constant for the 1s2s2p<sup>2</sup>3p <sup>6</sup>P<sup>o</sup>–1s2p<sup>3</sup>3p <sup>6</sup>P transitions for nuclear charges  $Z = 8, 9$  and  $10$ . The MCHF, SCHF, MCDF and the non-relativistic

SCHF differences are linear for nuclear charges  $Z = 8, 9$  and  $10$ . The MCHF difference for oxygen is  $226 \text{ cm}^{-1}$ .

In figure 6 the SCDF and the non-relativistic SCHF differences are constant for the  $1s2s2p^23p \ ^6S^o-1s2p^33p \ ^6P$  transitions for nuclear charges  $Z = 8, 9$  and  $10$ . The MCHF, MCDF and SCHF differences are linear for nuclear charges  $Z = 8, 9$  and  $10$ . The SCHF difference for oxygen is  $105 \text{ cm}^{-1}$ . However, SCDF, MCHF and SCDF differences are quite large,  $>4000 \text{ cm}^{-1}$  for nuclear charges  $Z = 8, 9$  and  $10$ . In [27] energy differences for the transitions related to multiplet S states also show the same tendency. The above linear and constant energy differences can be used to predict easily and with high accuracies the transition energies for the  $1s2s2p^23p \ ^6L^o-1s2p^33p \ ^6P$ , L = S, P, D, transitions for boronlike ions with  $5 < Z < 13$ .

The QED and the higher-order corrections for the  $1s2s2p^23p \ ^6L^o-1s2p^33p \ ^6P$ , L = D, P and S, transitions in O IV, F V and Ne VI are in the range of  $-220-370 \text{ cm}^{-1}$  (see tables 1, 2 and 3). We plot the QED and the higher-order corrections to the mean  $1s2s2p^23p \ ^6L^o-1s2p^33p \ ^6P$ , L = D, P, and S, transition energies in figure 7. Here, the QED and the higher-order corrections are calculated from the  $Z_{\text{eff}}$  values obtained from the SCHF and the MCHF results. For the  $1s2s2p^23p \ ^6L^o-1s2p^33p \ ^6P$ , L = D, P, and S, transitions in O IV, F V and Ne VI, the QED effects increase with  $Z$  rapidly. The results in figure 7 show that the mean transition wavelengths are sensitive to the QED effects to  $0.18 \text{ \AA}$ ,  $0.21 \text{ \AA}$  and  $0.22 \text{ \AA}$  for the  $1s2s2p^23p \ ^6L^o-1s2p^33p \ ^6P$ , L = D, P, and S, transitions in O IV, F V and Ne VI. They are at the same level or larger than the estimated experimental precision of  $\pm 0.06 \text{ \AA}$ ,  $\pm 0.10 \text{ \AA}$  and  $\pm 0.05 \text{ \AA}$ .

Some spectral lines of the boronlike ions remain unidentified. In the spectra in figures 2(b) and (c) several notable lines at  $666-668 \text{ \AA}$  show stable characteristics. Intensities measured at different ion energies indicate the features should be classified as transitions from upper states with doubly excited cores.

## 5. Conclusions

The fast beam-foil spectroscopic experiments have yielded new information on doubly excited sextet states in boronlike O IV, F V and Ne VI. We performed the MCHF (with QED and higher-order corrections) and the MCDF calculations for the  $2s-2p$  transitions between doubly excited sextet states in five-electron O IV, F V and Ne VI. Using the calculated wavelengths and transition rates, we were able to identify the observed lines in the fast beam-foil spectra of oxygen, fluorine and neon corresponding to the  $1s2s2p^23p \ ^6L^o-1s2p^33p \ ^6P$ , L = S, P, D, electric-dipole transitions in O IV, F V and Ne VI, and to measure the wavelengths with good accuracies. The measured results are compared with the values of the MCHF and MCDF calculations. The measured results and the calculated values are in reasonable agreement. To extract the QED and the higher-order corrections, accurate electron correlation is required.

## References

- [1] Lin B, Berry H G, Shibata T, Livingston A E, Garnir H P, Bastin T, Désevelles J and Savukov I 2003 *Phys. Rev. A* **67** 062507
- [2] Blanke J H, Fricke B, Heckmann P H and Träbert E 1992 *Phys. Scr.* **45** 430
- [3] Lapierre L and Knystautas E J 2000 *J. Phys. B: At. Mol. Opt. Phys.* **33** 2245
- [4] Miecznik G, Brage T and Fischer C F 1992 *Phys. Scr.* **45** 436
- [5] Berry H G, Bastin T, Biemont E, Dumont P D and Garnir H P 1975 *Rep. Prog. Phys.* **5** 12
- [6] Kramida A E, Bastin T, Biemont E, Dumont P D and Garnir H P 1999 *J. Opt. Soc. Am. B* **16** 1966
- [7] Chung K T 1984 *Phys. Rev. A* **29** 682

- [8] Fischer C F, Brage T and Jonsson P 1997 *Computational Atomic Structure an MCHF Approach* (Bristol: Institute of Physics Publishing)
- [9] Dyall K G and Grant I P 1989 *Comput. Phys. Commun.* **55** 425
- [10] Parpia F A, Fischer C F and Grant I P 1996 *Comput. Phys. Commun.* **94** 249
- [11] Fritzsche S and Grant I P 1997 *Comput. Phys. Commun.* **103** 277
- [12] Chung K T, Zhu X W and Wang Z W 1992 *Phys. Rev. A* **47** 1740
- [13] Chung K T and Zhu X W 1993 *Phys. Rev. A* **48** 1944
- [14] Drake G W F and Swainson R A 1990 *Phys. Rev. A* **41** 1243
- [15] Berry H G, Brooks R L, Cheng K T, Hardis J E and Ray W 1982 *Phys. Scr.* **42** 391
- [16] Hardis J E, Berry H G, Curtis L G and Livingston A E 1984 *Phys. Scr.* **30** 189
- [17] Garnir H P, Baudinet-Robinet Y and Dumont P D 1988 *Nucl. Instrum. Methods Phys. Res. B* **31** 161
- [18] Baudinet-Robinet Y, Dumont P D and Garnir H P 1990 *Phys. Mag.* **12** 3
- [19] Girardeau R, Knystautas E J, Beauchemin G, Neveu B and Drouin R 1971 *J. Phys. B: At. Mol. Phys.* **4** 1743
- [20] Bockasten K and Johansson K B 1968 *Ark. Fys.* **38** 563
- [21] Pettersson S G 1982 *Phys. Scr.* **26** 296
- [22] Moore C E 1965–1983 NSRDS-NBS 3 Section 1–10
- [23] Moore C E 1971 Atomic energy levels *Natl. Stand. Ref. Data Ser.* vols 1–3 (US National Bureau of Standards) (Reprint of *NBS Circ.* 467, originally issued in 1949, 1952 and 1958)
- [24] Engström L 1985 *Phys. Scr.* **29** 113
- [25] Brown R T 1969 *Astrophys. J.* **158** 829
- [26] Vainshtein L A and Safronova U I 1985 *Phys. Scr.* **31** 519
- [27] Blanke J H, Fricke B, Sepp W-D, Heckmann P H, Möller G and Wagner C 1990 *Phys. Scr.* **42** 522